ANTIOXIDANTS & REDOX SIGNALING
Volume 14, Number 3, 2011

DOI: 10.1089/ars.2010.3134

ORIGINAL RESEARCH COMMUNICATION

Silymarin: A Novel Antioxidant with Antiglycation and Antiinflammatory Properties *In Vitro* and *In Vivo*

Chi-Hao Wu, Shang-Ming Huang, and Gow-Chin Yen

Abstract

The current study was designed to evaluate the effects of silymarin (SM) on advanced glycation endproduct (AGE) formation and monocyte activation induced by S100b, a specific ligand of receptor for AGEs. The *in vivo* verification of antiglycation, antioxidant, and antiinflammatory capacities was examined by 12 weeks of SM administration in streptozotocin-diabetic rats. *In vitro* glycation assays demonstrated that SM exerted marked inhibition during the late stages of glycation and subsequent crosslinking. Dual action mechanisms, namely, antioxidant and reactive carbonyl trapping activities, may contribute to its antiglycation effect. SM produced a significant decrease in monocytic interleukin-1β and COX-2 levels and prevented oxidant formation caused by S100b, which appeared to be mediated by inhibition of p47phox membrane translocation. Chromatin immunoprecipitation demonstrated that S100b increased the recruitment of nuclear factor-kappaB transcription factor as well as cAMP response element-binding–binding protein and coactivator-associated arginine methyltransferase-1 cofactors to the interleukin-1β promoter, whereas these changes were inhibited with SM treatment. *In vivo*, SM reduced tissue AGE accumulation, tail collagen crosslinking, and concentrations of plasma glycated albumin. Levels of oxidative and inflammatory biomarkers were also significantly decreased in SM-treated groups compared with the diabetic group. These data suggest that SM supplementation may reduce the burden of AGEs in diabetics and may prevent resulting complications. *Antioxid. Redox Signal.* 14, 353–366.

Introduction

Diabetes is a life-long disease marked by elevated blood sugar levels. A significant factor associated with hyperglycemia is the resultant nonenzymatic glycation of biological proteins (3, 5), with the irreversible formation of advanced glycation end products (AGEs) (31, 34). This process occurs *in vivo* through the covalent binding of aldehyde or ketone groups of reducing sugars to free amino groups of proteins, forming AGE structures with a yellow-brown color and fluorescence. The AGEs have a propensity to generate reactive oxygen species (ROS) (2). In addition, glucose and other aldehydes, whether free or bound to protein, undergo auto-oxidation reactions to yield radicals and other reactive intermediates (*e.g.*, H_2O_2 and other peroxides), which can also contribute to the formation of AGEs. These latter processes are often termed glycoxidation (41).

Acute exposure to hyperglycemia induces reversible oxidative stress and circulating monocyte activation. Natarajan and colleagues (12, 35, 36) have suggested that high glucose levels and AGEs can generate large amounts of proinflammatory cytokines, such as tumor necrosis factor-α (TNF-α), interleukin-1β (IL-1β), and chemokines, including MCP-1 and IP-10. These inflammatory responses were found to be related to the modulation of signaling molecules, such as protein kinase C, p47phox, and/or mitogen-activated protein kinases, through oxidant stress-dependent or independent pathways. These pathways, in turn, control the activation of the nuclear factor-kappaB (NF-κB) transcription factor, thereby influencing the synthesis and expression of downstream inflammatory mediators. Antioxidants, such as α-tocopherol (40) or natural polyphenols (45), inhibit the aforementioned formation of ROS and cytokines as well as postpone inflammation.

The administration of supplemental antioxidants in response to the inhibition of protein modifications is a theoretical strategy for preventing diabetic complications correlated with glycooxidative stress (1). This hypothesis has been supported by clinical results that the development of diabetes and accumulation of AGEs may be reduced by the intake of natural antioxidants in the diet (26). Fruits, vegetables, and beverages are important dietary sources of flavonoids. Flavonoids are of current interest in research due to their important biological and pharmacological properties, particularly their antioxidant components (22). The flavonoid blend, silymarin (SM), is an extract from milk thistle (*Silybum*

Department of Food Science and Biotechnology, National Chung Hsing University, Taichung, Taiwan.

marianum L.) and is composed mainly of the following components: silybin A and B; isosilibybin A and B; silychristin; and silydianin. These flavonolignans are well known for displaying a remarkable spectrum of biological processes, including antioxidant, cytoprotective, and anticarcinogenic activities. In addition to its free radical scavenging properties, SM has been clinically used for its beneficial effects on various hepatic diseases where the pathogenesis involves an inflammatory response (47).

To date, studies of protein glycation (Maillard reaction *in vivo*) contribution to diseases have primarily focused on its relationship to diabetes and diabetes-related complications (17). However, there is no relevant information determining if phytochemicals offer protective effects that guard against glycotoxin-induced damage. This study is the first to report SM as a promising inhibitor of protein glycation for the prevention of oxidative and inflammatory injury against AGEs *in vitro* and *in vivo*, providing evidence to support the health benefits of milk thistle for diabetic patients. Considering that SM behaves similarly to aminoguanidine (AG), which was the first inhibitor of AGEs investigated in clinical trials, it has great potential to be used as an agent to alleviate diabetic complications without adverse side effects.

Materials and Methods

Chemicals and reagents

AG, *N*-acetyl-glycyl-lysine methyl ester (G.K.) peptide, bovine serum albumin (BSA; fraction V, essentially fatty acid free), δ-gluconolactone (δ-Glu), methylglyoxal (MG), phenyl-*tert*-butyl-nitron, S100b (bovine brain), SM, and streptozotocin (STZ) were purchased from Sigma Chemical Co. An anti-AGE monoclonal antibody (6D12) was purchased from Trans Genic, Inc. Antibodies to p47phox and β-actin were obtained from Cell Signaling Technology. The antiepidermal growth factor receptor antibody was obtained from Santa Cruz Biotechnology. Anti-p65, anticoactivator-associated arginine methyltransferase-1 (CARM1), anti–CAMP response element-binding (CREB)-binding protein (CBP), antiacetyl-histone H3 (acetyl-histone 3 [HH3] that recognizes Lys9 and Lys14), antimethylated histone H3 at Arg17 (methyl-HH3R17), and anti-receptor for AGE (RAGE) antibodies were obtained from Upstate Biotechnology, Inc. The pharmacological inhibitor specific for NADPH oxidase (apocynin [APO]) was obtained from Biosource. Immunohistochemical reagents were obtained from DakoCytomation. All of the chemicals and solvents used were of analytical grade.

Assays for individual stages of protein glycation

Early stages of protein glycation were determined with a hemoglobin-δ-Glu assay (32). This method is specifically devised for the investigation of inhibitors of the formation of Amadori products, as evidenced by decreased glycated hemoglobin (HbA_{1C}) levels. A BSA-glucose assay was used to evaluate the ability of SM to inhibit glucose-mediated protein glycation, and the development of AGE-related fluorescence was measured according to the method described by Wu and Yen (43). A G.K. peptide-ribose assay was used to evaluate the ability of SM to inhibit the crosslinking of G.K. peptides (late glycation products) in the presence of ribose using the method described by Nagaraj *et al.* (28) and Rahbar *et al.* (32). To evaluate the reactive carbonyl trapping activity, the inhibition of MG-mediated protein crosslinking and aggregation by SM was determined by sodium dodecyl sulphate-polyacrylamide gel electrophoresis (SDS-PAGE) in a BSA-MG model (43). AG, an established anti-AGE agent (39), was used as a positive control.

Determination of free radicals generation by electron spin resonance

Free radical generation was measured according to the methods described by Finotti *et al.* (10). Electron spin resonance (ESR) spectra were measured on glycated samples (BSA-glucose assay) with a reaction mixture containing 0.2 mM phenyl-*tert*-butyl-nitron. The ESR spectra were recorded on a Bürker (EMX-10/12) spectrometer under previously described conditions (43). No ESR signals were detected in any of the reagents used in the ESR analysis. All spectra were recorded at room temperature.

Cell culture and treatments

The human acute monocyticleukemia cell line (THP-1) was obtained from the Bioresource Collection and Research Center (BCRC 60430; Food Industry Research and Development Institute) and was cultured in glucose-free RPMI 1640 medium (Gibco BRL, 11879-020) supplemented with 10% FBS, HEPES (10 mM), streptomycin (100 μg/ml), penicillin (100 U/ml), 50 μM β-mercaptoethanol, and 5.5 mM D-glucose (normal glucose, NG) in a 5% CO_2 incubator at 37°C. For AGE challenge experiments, S100b protein (6.5 μg/ml), a specific RAGE ligand, was given to cells for 4 h with or without SM. The cell viability test was determined by a Trypan blue dye exclusion assay. With NG culture conditions, SM had no cytotoxicity on THP-1 monocytes at a concentration range of 5–25 μg/ml (cell viability >95%; data not shown).

RNA preparation and quantitative real-time polymerase chain reaction

Total RNA was prepared from THP-1 cells (1×10^6 cells/ml) by a Trizol RNA isolation kit, as described in the manufacturer's manual. From each sample, 1 μg of RNA was reverse transcribed to cDNA using SuperScript III First-Strand Synthesis SuperMix for qRT-PCR kit (Invitrogen). Polymerase chain reaction (PCR) analyses were performed to detect IL-1β and COX-2 gene expression in THP-1 cells using a PCR Master Mix 2× kit (Fermentas, Glen Burnie, MD). Multiplex PCRs were performed for 29–35 cycles by using a P×2 Thermal cycler (Thermal Electron Co.). The qRT-PCR primers were as follows: IL-1β, forward (5′-CTCTCTCACCTCTCCTACTCAC-3′) and reverse (5′-ACACTGCTACTTCTTGCCCC-3′); COX-2, forward (5′-ATCT ACCCTCCTCAAGTCCC-3′) and reverse (5′-TACCAGAAG GGCAGGATACAG-3′); β-actin, forward (5′-ACAAAACCTA ACTTGCGCAG-3′) and reverse (5′-TCCTGTAACAACGCAT CTCA-3′). PCR products were fractionated on 1.8% agarose gels, and the signals were detected using SYBR DNA staining (Invitrogen). For quantification, the PCR bands on the gel photograph of the gel were scanned using a densitometer linked to a computer analysis system. After normalizing the gene signal relative to the corresponding β-actin signal from each sample, the results were expressed as fold stimulation over S100b.

Western blotting

The membrane protein fractions were extracted by a compartmental protein extraction kit. Western blotting was performed as previously described (45). Antibodies against p47phox and epidermal growth factor receptor were used. The relative protein expression was quantified densitometrically using LabWorks 4.5 software and was calculated in relation to the loading control reference band.

Measurement of monocytic IL-1β release and ROS production

THP-1 cells were incubated in NG medium with 0.2% BSA. The cells were challenged with S100b (6.5 μg/ml) and either with or without SM for 4 h. The supernatant-conditioned medium was then harvested and assayed for IL-1β secretion using a specific ELISA kit according to the manufacturer's instructions (Pierce Endogen). The pure medium (without cells) was incubated under the same conditions and was used as a blank control for the ELISA. Intracellular ROS generation was detected using a fluorescent probe, 5-(and-6)-carboxy-2′,7′-dichlorodihydro-fluorescein diacetate (DCFH-DA) (Molecular Probes, Eugene, OR), as previously described (45).

Chromatin immunoprecipitation assays

Chromatin immunoprecipitation (ChIP) assays were performed with an EZ-ChIP™ chromatin immunoprecipitation kit (Millipore) according to the manufacturer's instructions. Briefly, THP-1 cells (1×10^7 cells/ml) were crosslinked with 1% formaldehyde and then sheared with 4–5 sets of 10 s pulses using a Misonix sonicator ultrasonic processor (model XL2020) set to 30% of maximal power. One-tenth of the total lysate was used for total genomic DNA as an Input DNA control. Immunoprecipitation was performed overnight with 5–10 μg each of specific antibodies. Precipitates were washed and extracted with 1% SDS containing 0.1 M $NaHCO_3$. Elutes were pooled and heated to 65°C for 5 h to reverse protein/DNA crosslinked complexes to free the DNA. The DNA fragments were purified with spin columns. For PCR, 2 μl of the DNA sample was used. The PCR primers correspond to sequences within the promoter regions as follows: IL-1β, forward (5′-CACTCTTCCACTCCCTCC-3′) and reverse (5′-AGCCTCAAACCCTTCCTC-3′); TNF-α, forward (5′-CCCT CCAGTTCTAGTTCTATC-3′) and reverse (5′- GGGGAAA GAATCATTCAACCAG-3′); COX-2, forward (5′- CAAGGC GATCAGTCCAGAAC-3′) and reverse (5′- GGTAGGCTT TGCTGTCTGAG-3′).

Animals and experimental procedure

Experimental diabetes was induced in male Sprague Dawley rats (200 ± 10 g) by i.p. injection of STZ (55 mg/kg diluted in 0.1 mol/L citrate buffer at pH 4.5) after an overnight fast according to the methods described by Forbe *et al.* (11). Sham-injected control animals (0.1 mol/L citrate buffer at pH 4.5) were followed concurrently. Only animals with a plasma glucose concentration more than 15 mmol/L 1 week post-induction of diabetes were included in the study as being diabetic. The experimental animals were randomly divided into five groups where each group contained 8 to 10 rats. Group I was the nondiabetic control (NC), whereas group II was the diabetic control (DC). These two groups were only fed the basal diet. Group III consisted of DC rats that were treated with a diet containing 0.3% (w/w) AG. Groups IV and V consisted of the DC rats that were treated with a diet containing 0.1% SM (SM-L) and 0.3% SM (SM-H) SM, respectively. The doses of SM and AG administered to experimental animals used were estimated from food consumption of 5% of body weight per day. For example, the estimated dosage of SM-H groups for a 300 g rat was as follow: 15 g/day×0.3% 150 mg/kg body weight/day.

All animals were housed individually in an air-conditioned room maintained at 25°C ± 1°C with 55%–60% humidity and a 12-h light/dark cycle. Sterilized water was accessible *ad libitum*. Treatments commenced from the seventh day after STZ or control vehicle injection and continued for 12 weeks. Body weights and fluid intake were recorded daily, and blood glucose levels were monitored weekly throughout the study. At the end of the experiments, the rats were sacrificed after an overnight fasting and blood was withdrawn from the abdominal aorta under diethyl ether anesthesia. The blood samples were later centrifuged (1500 *g* for 10 min at 4°C) for plasma isolation. The aorta and kidney were immediately collected, rinsed in ice-cold PBS, and weighed. The specimens were then snap-frozen in liquid nitrogen or fixed in 10% (v/v) formalin for further immunohistochemical analyses. All experimental procedures involving animal studies were conducted in accordance with the National Institute of Health (NIH). This experiment was approved by the Institutional Animal Care and Use Committee of the National Chung Hsing University, Taichung, Taiwan.

Tissue extraction

The method used for tissue extraction was previously reported (42). Briefly, aorta and renal samples (100 mg) were homogenized with 1 ml of RIPA buffer (Cell Signaling Technology). Tissue proteins were prepared by the addition of 1 ml of 50% (w/v) trichloroacetic acid to the homogenated samples and were centrifuged at 20000 *g*. The resulting pellets were recovered and washed with diethyl ether before drying. The drying pellets were dissolved in sample buffer for subsequent identification analysis using SDS-PAGE. The aorta and renal AGEs were measured by immunoblot using an anti-AGE antibody as described above. The relative expression of protein was quantified densitometrically using LabWorks 4.5 software and was calculated in relation to the reference band of the loading control.

Immunohistochemical detection of AGEs

For immunohistochemical AGE staining, formalin-fixed, paraffin-embedded section cuts (2 μm thick) were mounted on slides coated with 2-aminopropyltriethoxy silane, baked for 3 h at 58°C, deparaffinized, rinsed with 3% H_2O_2, and incubated with proteinase K (0.5 mg/ml) for 5 min at room temperature as previously described (8). These sections were washed with rinse buffer and blocked with StartingBlock™ blocking buffers (Pierce) for 5 min and subsequently incubated with an anti-AGE monoclonal antibody (6D12) for 30 min. After washing with rinse buffer, the sections were incubated with EnVision + labeled polymer peroxidase-conjugated anti-IgG for 30 min at room temperature, followed by detection with a 3,3-diaminobenzidine tetrahydrochoride solution (chromogen) and hematoxylin (counterstain).

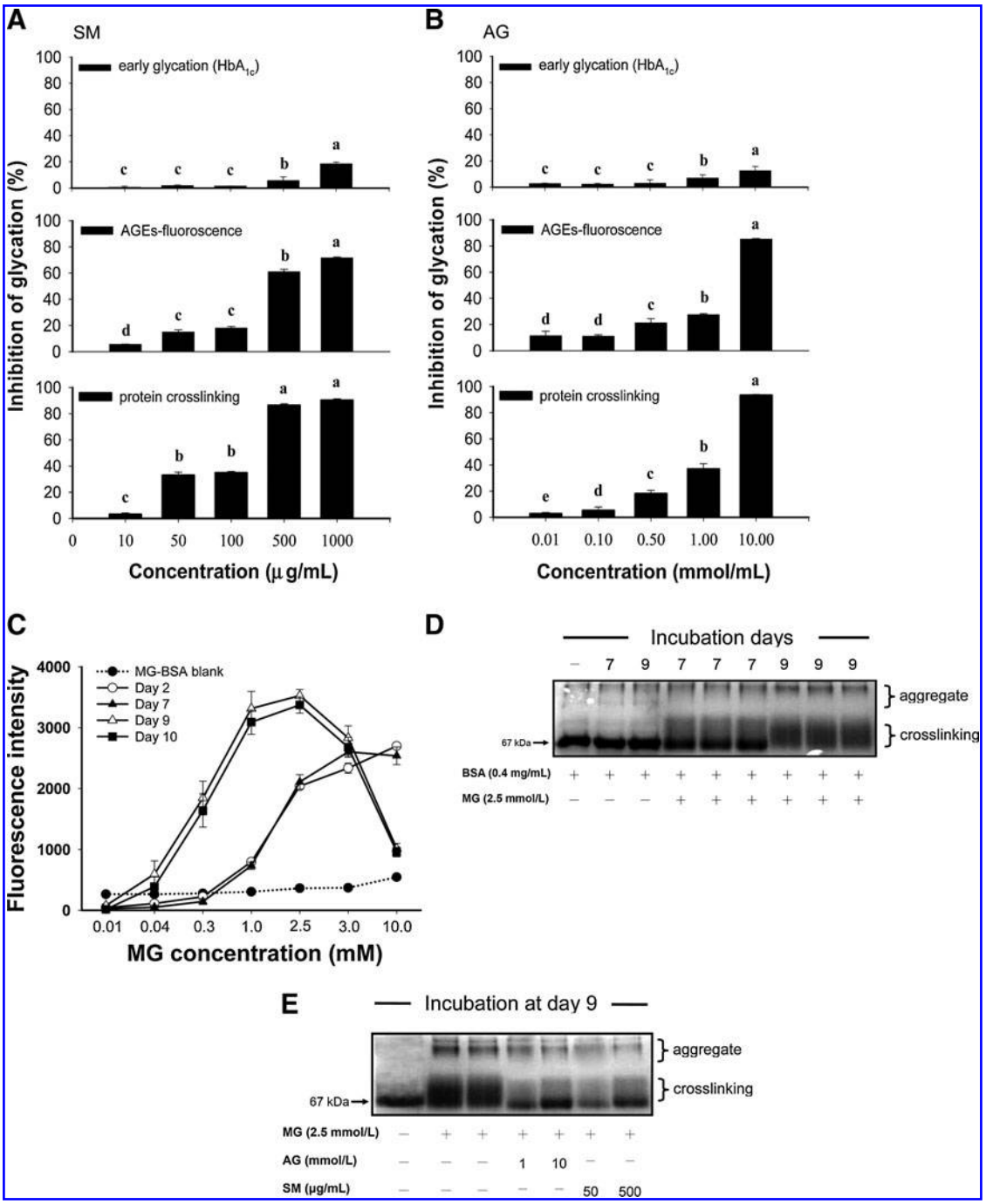

FIG. 1. Effects of SM and AG on *in vitro* protein glycation and formation of AGEs. Dose responses of glycation inhibition (%) of SM (**A**) on individual stages of protein glycation were determined by model systems of δ-Glu assay (*upper panel*), BSA-glucose assay (*middle panel*) and *N*-acetyl-glycyl-lysine methyl ester peptide-ribose assay (*bottom panel*) and were compared with responses of AG (**B**). Data are the means ± SD for $n = 6$. Groups with different letters are significantly different ($p < 0.05$). (**C**) Time–response curves of MG-mediated development of fluorescence of glycated BSA. Fluorescence of the samples was measured at the excitation and emission wavelengths of 350 and 450 nm, respectively. (**D**) The modulation of MG-mediated protein modification is shown by sodium dodecyl sulphate-polyacrylamide gel electrophoresis. (**E**) Inhibition of protein aggregates and crosslinking by SM or AG after 9 days of incubation with MG and BSA. The first left lane is BSA alone (blank: unglycated protein); lanes 2–3 are MG controls (glycated protein); lanes 4–5 are AG treatments; lanes 6–7 are SM treatments. AGEs, advanced glycation end products; BSA, bovine serum albumin; AG, aminoguanidine; MG, methylglyoxal; SM, silymarin.

Measurement of glycative parameters in experimental rats

HbA_{1c} and urinary albumin excretion were examined by the Union Clinical Laboratory (Taichung, Taiwan). Determination of AGE-related fluorescence was based on spectrofluorimetric detection according to Münch *et al.* (27) with slight modifications. Briefly, blood serum was diluted (1:50) with PBS (pH 7.4), and the fluorescence intensity was detected with a FLUOstar galaxy fluorescence plate reader (BMG Labtechnologies) with an excitation wavelength of 370 nm and emission wavelength of 440 nm. The fluorescence intensity was expressed in arbitrary units (AU). Plasma-glycated albumin levels were estimated with Glycalbumin ELISA kits (GAR-50; Exocell, Inc.) using a monoclonal antibody (A717) that specifically recognizes the glycated moieties in glycated albumin. Glycated albumin values were expressed relative to total albumin content after determination of total plasma albumin. Intraassay and interassay precision for samples within the useful range of the assay had a C.V. within 10% of the mean. Analysis of tail tendon breaking time was assessed according the method described by Yue *et al.* (48). Collagen fibers were cut in 5 cm lengths weighing 2–2.5 mg. The mean breaking time was taken as tendon breaking time.

Measurement of oxidative biomarkers in experimental rats

The levels of 8-isoprostane in the plasma were examined with a commercial ELISA kit (Cayman Chemical Corporation) following the manufacturer's protocol. Carbonyl proteins were analyzed by the determination of absorbance (14). The concentration of carbonyl groups was calculated using the absorbance of 1 nmol/ml of carbonyl at $365 = 0.021$. The data were expressed as the amount in nanomoles of carbonyl protein formed per milligram of total protein. The determination of erythrocyte oxidative hemolysis was performed with [2,2-azobis(2-amidinopropane)dihydrochloride]-derived peroxyl radicals as previously described (37). DNA damage of peripheral blood lymphocytes in rats was determined by Comet assay according the methods previously described by Wu *et al.* (44). The slides were examined on a Nikon EFD-3 fluorescence microscope with excitation filter BP at 543/10 nm and a 590-nm emission barrier filter. Objective measurements of the distribution of DNA were performed for a sample of cells using Komet 3.1 software (Kinetic Imaging Ltd.). One hundred cells on each slide (scored at random) were classified according to the relative intensity of the fluorescence in the tail. The degree of DNA damage was scored by determining the percentage of DNA in the tail as follows: Tail DNA% = [Tail DNA/(Head DNA + Tail DNA)]×100.

Measurement of inflammatory mediators in experimental rats

Plasma TNF-α levels were estimated with an ELISA kit according to the manufacturer's instructions (Pierce Endogen). Nitric oxide (NO) release was determined spectrophotometrically by measuring the accumulation of its stable degradation products, nitrite and nitrate, according to the methods previously described (15). Briefly, the fresh plasma was treated with a $ZnSO_4$ and Cd suspension. After centrifugation, the supernatant was incubated with 1% sulfonamide and 0.1% naphtylethylenediamine for 10 min at 60°C. The absorbance at 546 nm was measured with a spectrophotometer, and the results were expressed in nanomolar units.

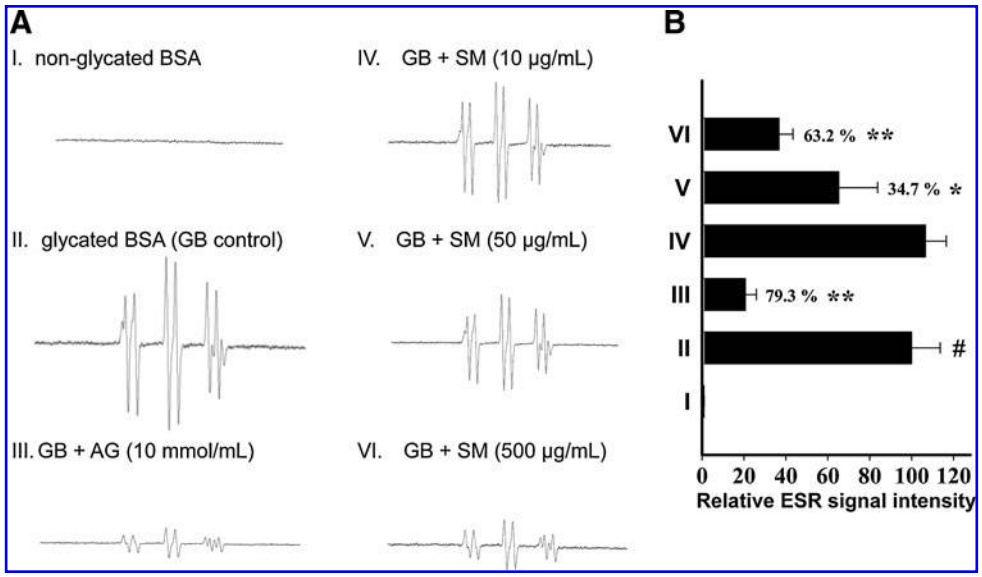

FIG. 2. ESR spectra of nonglycated and GB in the absence and presence of AG or SM using the spin trap phenyl-*t*-butyl-nitron. (**A**) ESR spectra were measured on glycated samples with a reaction mixture containing 0.2 mM phenyl-*tert*-butyl-nitron. The ESR spectra were recorded on a Bürker (EMX-10/12) spectrometer (Karlsruhe, Germany) with the following conditions: incident microwave power, 20.117 mW; frequency, 9.722 GHz; modulation amplitude, 1.50 G; modulation frequency, 100.00 kHz; time constant, 163.84 ms; sweep time, 167.77 s; receiver gain, 1.00×10^{-5}; sweep width, 100.00 G; field center, 3300.00 G. No ESR signals were detected in any of the reagents used in the ESR analyses. All spectra were recorded at room temperature. The following groups are shown above: (I) nonglycated BSA; (II) GB control; (III) GB with AG (10 mmol/L); (IV) GB with SM (10 μg/ml); (V) GB with SM (100 μg/ml); (VI) GB with SM (500 μg/ml). (**B**) The graph represents quantitative data of relative EPR signal intensity (%) as estimated by WINEPR SimFonia software (Version 1.25). The scavenging effects were calculated as follows: scavenging effects (%) = 100 − relative ESR signal intensity (%). $^{\#}p < 0.05$ compared with non-glycated BSA. $^{*}p < 0.05$ and $^{**}p < 0.01$ are significantly different by comparison with GB control (II). Values in the column are percent inhibition of free radicals derived from GB. Data are presented as the means ± SD from three independent experiments. ESR, electron spin resonance; GB, glycated BSA.

Statistical analysis

Each experiment was performed in triplicate. The results were expressed as the means ± SD. Statistical comparisons were made by one-way analysis of variance, followed by a Duncan multiple-comparison test. Differences were considered significant when the p-values were <0.05.

Results

Effects of SM on individual stages of protein glycation

The effects of SM on individual stages of protein glycation are demonstrated in Figure 1A and were compared with the effects of AG (Fig. 1B), an established AGE inhibitor. Three assay methods were adopted to evaluate the antiglycation effects of SM as follows: (a) δ-Glu assay, which is an assay based on inhibition of the Amadori product (HbA_{1c} levels) generated during early stages of protein glycation (32); (b) BSA-glucose assay, which is an assay based on AGE-related fluorescence generated in the course of glycation (45); and (c) G.K. peptide-ribose assay, which is an assay based on the inhibition of protein-AGE crosslinking (28, 32). The results demonstrated that SM and AG had only a moderate inhibitory effect on the early stages of glycation (Fig. 1A, B, upper panel), whereas SM exerted marked inhibitory effects on late glycation, AGE formation (Fig. 1A, B, middle panel), and the subsequent protein crosslinking (Fig. 1A, B, bottom panel). As a result, SM is likely to behave in a similar fashion as AG in inhibiting protein glycation.

MG, a reactive carbonyl species (RCS), readily reacts with protein lysine and arginine protein residues to produce high-molecular-weight, cross-linked products (19, 28, 38). Time- and dose-dependent effects of MG-mediated protein glycation were determined by AGE-related fluorescence and SDS-PAGE protein maps. MG at a concentration of 2.5 mmol/L developed the most significant fluorescence after an incubation period of 9 days (Fig. 1C). There was a decrease in the detectable amount of BSA in its position at the bottom of the gel in addition to less resolution and spreading of bands compared with untreated protein (Fig. 1D). This result was similar to MG-treated BSA and ovalbumin as previously described (19). When SM (50 and 500 μg/ml) or AG (1 and 10 mmol/L) were present in the incubation mixture, losses of BSA and the formation of the high-molecular-weight protein were suppressed (Fig. 1E). This was an indication of SM- and AG-mediated *in vitro* protection against glycation. As mentioned above, AG has been demonstrated as an antioxidant and nucleophilic agent, possessing a potent scavenging effect on highly RCS (39). Thus, it is speculated that SM may exhibit an RCS trapping effect.

Scavenging activity of SM on glycation-derived free radicals

ROS are involved in the Maillard reaction, and that the formation of free radicals occurs during the glycation process (13, 33). On the basis of the significant inhibitory effect of SM against *in vitro* glycation (Fig. 1), ESR spectrometry was utilized to investigate the scavenging effect of SM on glycation-derived radicals. The ESR spectra clearly showed that protein glycation led to increased production of free radicals (Fig. 2A). The addition of SM to the reaction system caused a dose-dependent decrease in the ESR signal intensity (Fig. 2B), indicating that SM-mediated glycation inhibition may be related to its antioxidant properties.

SM inhibited expression of inflammatory mediators in S100b-stimulated monocytes

The ligation of S100b to RAGE is an important part of complex interactions of the oxidative stress and inflammatory responses (7). S100b serves as a valuable tool in the study of AGE-RAGE signaling and the diabetic inflammatory conditions (9, 35). As shown in Figure 3A, S100b (6.5 μg/ml) treatment in THP-1 cells for 4 h resulted in an approximate three- to fourfold increase in mRNA expression levels of IL-1β and COX-2. Moreover, SM dose de-

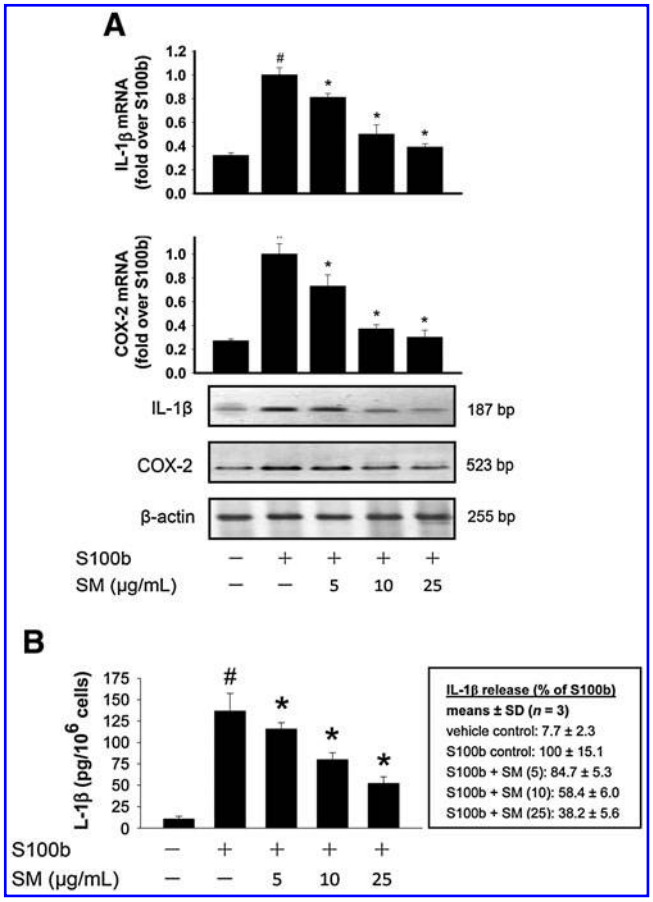

FIG. 3. Effect of SM on S100b-induced IL-1β and COX-2 activation in THP-1 monocytes. (**A**) Cells were cultured in normal glucose (NG; 5.5 mmol/L) medium with or without SM (5–25 μg/ml) for 4 h. Total RNA was isolated and analyzed for IL-1β and COX-2 mRNA expression by RT-polymerase chain reaction (PCR). The intensity of each gene-specific band was normalized to internal controls (β-actin). The results are expressed as multiples of S100b induction. (**B**) Cells treated with the same conditions were assayed for IL-1β production by ELISA as described in the Materials and Methods section. All appropriate controls and standards as specified by the manufacturer were used. The data are expressed as pg of IL-1β secretion per 1 million cells. Values shown are the means ± SD from three independent experiments. $^{\#}p < 0.05$ compared with NG (vehicle control). $^{*}p < 0.05$ compared with the S100b control. IL-1β, interleukin-1β.

pendently ($p < 0.05$) inhibited both the gene and protein levels of IL-1β in monocytes (Fig. 3).

Effect of SM on intracellular ROS production and p47phox translocation in monocytes

We next examined whether S100b induced a pro-oxidant status in cultured monocytes and estimated the protective effect of SM against intracellular ROS production. DCFH-DA staining showed that S100b-treated cells exhibited a striking increase in the basal levels of ROS compared with NG control cells (Fig. 4A, B; $p < 0.05$). A significant reduction of ROS was observed after the treatment with SM (5–25 μg/ml, $p < 0.05$). Further, the S100b-driven ROS production was completely blocked by pretreatment with APO, an NADPH oxidase inhibitor, indicating that the activation of NADPH oxidase may have a role in the elevated levels of oxidative stress caused by S100b.

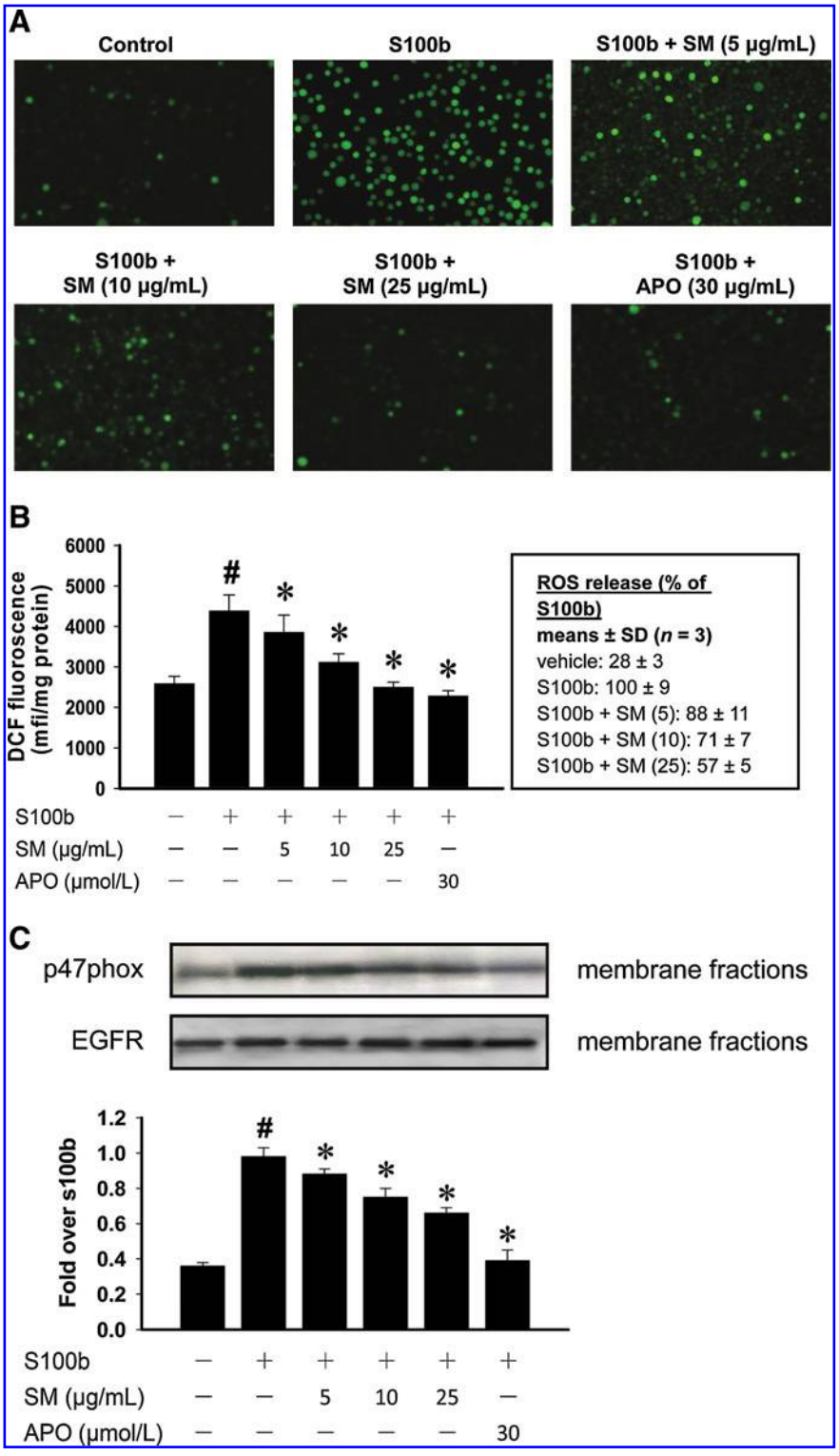

FIG. 4. Effect of SM on S100b-induced ROS generation and p47phox translocation in THP-1 monocytes. Cells were cultured in NG medium with or without SM (5–25 μg/ml) for 4 h. (**A**) Cells cultured in six-well plates were loaded with DCFH-DA (10 μmol/L) for 30 min. Cells were then washed with PBS three times, and live cells were imaged on an inverted fluorescence microscope. The images shown are representative of at least three independent experiments with similar results. (**B**) ROS generation was quantified using mfi with the fluorescent probe DCFH-DA as indicated in **A**. Values shown are the means ± SD from three independent experiments. $^{\#}p < 0.05$ compared with NG (vehicle control). $^{*}p < 0.05$ compared with the S100b control. (**C**) Membrane fractions of cell lysates were prepared after treatment with or without SM challenged by S100b. Proteins separated by sodium dodecyl sulphate-polyacrylamide gel electrophoresis were immunoblotted and probed with either an anti-p47phox antibody or anti-EGFR antibody as an internal control. To ascertain if the total level of each protein did not change, western blots were probed with an anti-p47phox antibody (*top panel*), stripped, and reprobed with an anti-EGFR antibody (*bottom panel*) to show equal loading. The extent of protein expression was expressed as multiples of S100b induction. Results shown are representative of three independent experiments. EGFR, epidermal growth factor receptor; mfi, mean fluorescent intensities; ROS, reactive oxygen species. DCFH-DA, 2′,7′-dichlorodihydro-fluorescein diacetate. (For interpretation of the references to color in this figure legend, the reader is referred to the web version of this article at www.liebertonline.com/ars).

Therefore, the effect of S100b on p47phox protein expression, an NADPH oxidase subunit, was investigated. As shown in Figure 4C, membrane translocation of p47phox was significantly increased in S100b-treated cells as compared with untreated control cells ($p < 0.05$), whereas the addition of SM inhibited these translocation events. Moreover, the S100b-induced p47phox translocation was also blocked by APO treatment. These results suggest that SM has a potent impact on intracellular ROS formation, and may be partly due to downregulation of the NADPH oxidase activities.

S100b increased the recruitment of NF-κB p65 to the IL-1β gene promoter in monocytes

Diabetic stimuli such as hyperglycemia (6, 12) and/or AGEs (22) augment expression of inflammatory genes by transcriptional mechanisms. We demonstrated with ChIP assays that S100b increased the binding of NF-κB p65 subunit to the promoter of the IL-1β gene in monocytes, and these nuclear events were significantly enhanced when cells were challenged with S100b (Fig. 5A). Little or no binding behavior was found in NG control cells and NG cells without the addition of a p65 antibody (Fig. 5A, lanes 1 and 2), indicating the specificity of the S100b effects. There was no change in the amplification of input DNA (loading control) in all cases (Fig. 5A, lower panel). In addition, the recruitment of p65 to the promoters of COX-2 and TNF-α was also observed (Fig. 5B).

To clarify the molecular transcription mechanisms and nuclear chromatin remodeling events of antiinflammatory activities, SM was examined with ChIP assays. The RAGE antibody was also included as a reference drug. As the results show in Figure 5C, the recruitment of p65, which was involved in S100b-stimulated IL-1β promoter activation, was blocked by RAGE antibody treatment (lane 4). At a concentration of 25 μg/ml, SM had a marked inhibitory effect against S100b-mediated p65 recruitment in monocytes (lane 3).

ChIP assays of coactivator recruitment and histone modifications in response to S100b stimulation in monocytes

A time course of S100b-induced recruitment of chromatin remodeling factors to the IL-1β promoter was performed with antibodies to CBP, CARM1, acetyl-HH3, and methyl-HH3R17 with ChIP assays. Figure 6A shows that (a) S100b increased the recruitment of the CBP and CARM1 coactivators to the IL-1β promoter as early as 15 min after S100b treatment; (b) acetylation of HH3 occurred as early as 15 min after S100b treatment and reached a plateau at a 60 min incubation period and decreased after 2 h; and (c) similar results were also obtained with a methylation of HH3 at Arg17, which reached a plateau at a 30 min incubation period and decreased after 1 h. The input DNA was not altered by the S100b treatment (Fig. 6A; lowest panel). Additional experiments revealed that SM actively abrogated the amounts of acetylated Lys residues and methylated Arg residues of HH3 within the IL-1β promoter in response to S100b stimulation (Fig. 6B). Our results indicated that S100b stimuli induced histone acetylation and methylation at specific Lys and Arg residues within the IL-1β gene. These results provide novel evidence that a close relationship exists between proinflammatory gene activation and acetylated and/or methylated histone accumulation under high glycotoxin conditions.

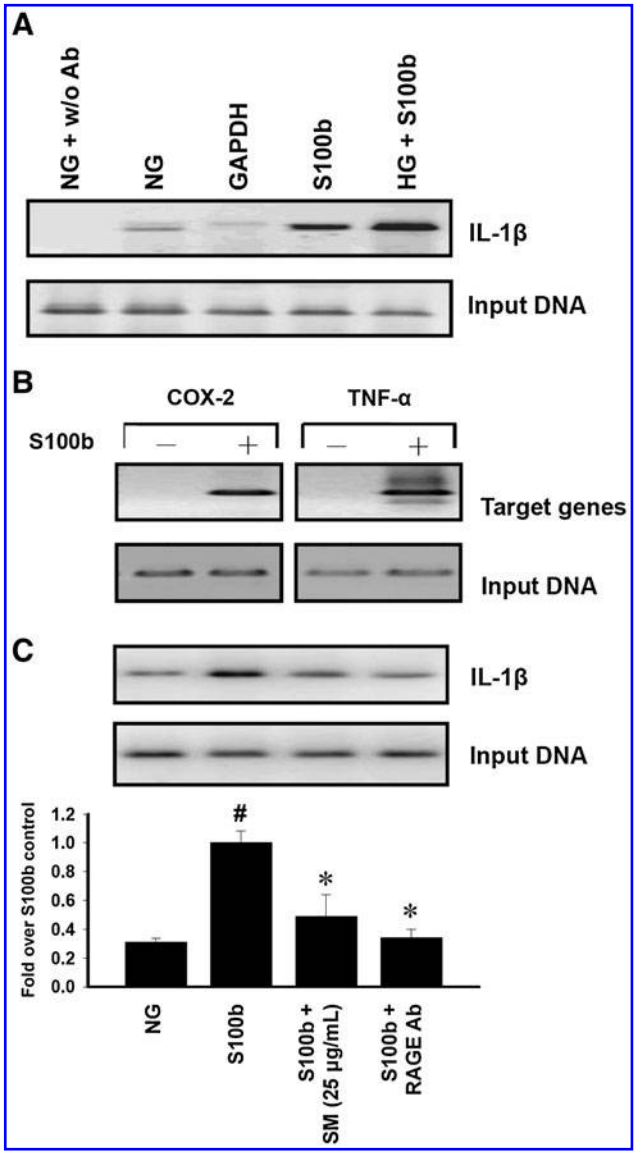

FIG. 5. ChIP assays of S100b-induced binding of nuclear factor-kappaB p65 at the inflammatory gene promoters in monocytes and the inhibitory effects of SM. THP-1 cells were cultured under NG or high-glucose (15 mmol/L) conditions for 30 min. Crosslinked chromatin samples were subjected to ChIP assays using antibodies specific to p65. PCRs were then performed with the immunoprecipitated DNA to amplify the IL-1β (**A**), COX-2 (**B**, *left panel*), and tumor necrosis factor-α (**B**, *right panel*) promoters around nuclear factor-kappaB sites as indicated in the Materials and Methods section. The *lower panel* shows the amplification of input DNA before immunoprecipitation. (**C**) SM and anti-RAGE antibody suppress the S100b-induced recruitment of p65 at the IL-1β gene promoter. THP-1 cells were cultured under NG conditions with or without SM as indicated in **A**, except that cells were pretreated with an anti-RAGE antibody (70 μg) for 1 h followed by challenged with S100b protein for 30 min. The extent of chromatin modifications was quantified and expressed as multiples of S100b induction (**C**, *lower panel*). Results shown are representative of three independent experiments. Ab, antibody; ChIP, chromatin immunoprecipitation; HG, high glucose; TNF-α, tumor necrosis factor-α; w/o, without. $^{\#}p < 0.05$ compared with NG (vehicle control). $^{*}p < 0.05$ compared with the S100b control.

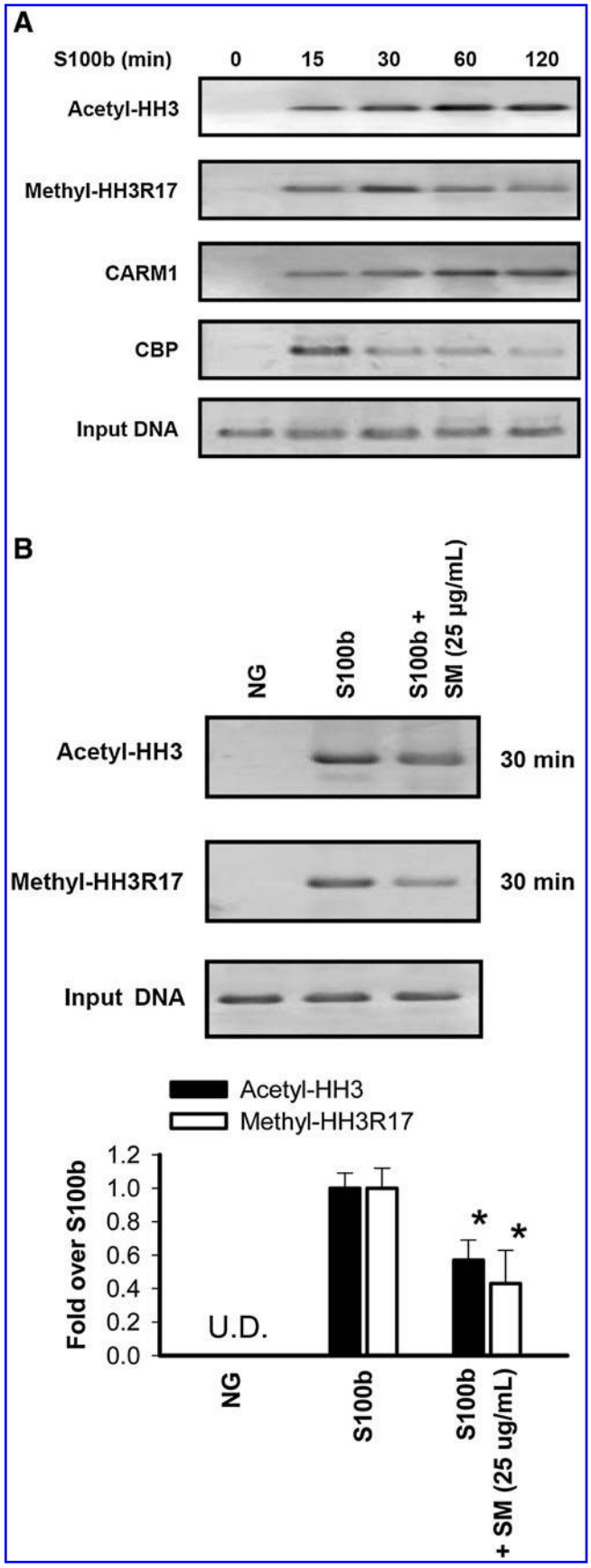

Physical and biochemical parameters in experimental rats

At 12 weeks, the DC group had a significant increase in blood glucose and HbA_{1c} levels compared with the levels in the NC group ($p < 0.05$ *vs.* DC group). However, no differences in glycemic levels were noted between treated and untreated diabetic groups (Table 1). The administration of SM-H (0.3% of diet) to rats showed only moderate hypoglycemic and urinary albumin excretion lowering effects that did not reach statistical significance ($p > 0.05$). Diabetic animals had decreased body weights but large increases in daily fluid intake indicating classic diabetes symptoms. No attenuation of these changes was demonstrated with AG or SM treatments (Table 1). In addition, normal rats treated with AG or SM did not show any differences from the NC group with respect to glycemic levels, body weights, or fluid intake ($p > 0.05$; data not shown).

Oxidative and inflammatory biomarkers in experimental rats

In vivo biomarkers of oxidative stress, such as 8-isoprostane, carbonyl groups, lymphocyte DNA damage, and erythrocyte hemolysis, were significantly increased in the DC group compared with the NC group ($p < 0.05$). These parameters were reduced in diabetic rats receiving SM-H (0.3% of diet) compared with untreated diabetic animals. No differences were observed in 8-isoprostane, lymphocyte DNA damage, and erythrocyte hemolysis in diabetic animals treated with SM-L. We also confirmed that treatment with AG resulted in a 26% reduction in lymphocyte DNA damage compared with the DC group (Table 1).

Levels of inflammatory mediators in plasma at the end of the 12-week experimental period are shown in Table 1. Diabetes found in the DC group was associated with a significant increase in plasma levels of TNF-α and NO compared with animals in the NC group. Treating the DC group with AG or SM-H reduced plasma TNF-α and NO levels, and to a lesser extent with animals in the SM-L group (Table 1).

FIG. 6. S100b induced histone modifications and chromatin remodeling at the promoter of IL-1β gene and the inhibitory effects of SM. (**A**) Time course of S100b-induced histone acetylation and methylation and the recruitment of CBP and CARM1 at the promoter of IL-1β. THP-1 cells were cultured under NG conditions in the presence or absence of S100b for various time periods. Crosslinked chromatin samples were subjected to ChIP assays using antibodies specific to acetyl-HH3 (recognizes Lys9 and Lys14 acetyl), HH3R17Me (recognizes Arg17 methyl), CBP, and CARM1, respectively. PCRs were then performed with the immunoprecipitated DNA to amplify the IL-1β promoter as indicated in the Materials and Methods section. The *lower panel* shows the amplification of input DNA before immunoprecipitation. (**B**) Effect of SM on S100b-induced histone acetylation and methylation at the promoter of IL-1β gene. Cells were treated with or without SM for 30 min and then ChIP assays performed with specific Abs as indicated in **A**. The extent of chromatin modifications was quantified and expressed as multiples of S100b alone. The lower panel shows the amplification of input DNA before immunoprecipitation. Results shown are representative of three independent experiments. CARM1, coactivator-associated arginine methyltransferase-1; CBP, CREB-binding protein; HH3, histone 3.

Table 1. Effects of Silymarin and Aminoguanidine on Physical and Biochemical Parameters, and the Biomarkers for Evaluating Oxidative Stress and Inflammation at Week 12 in Experimental Diabetic Rats

Parameters	*Nondiabetic control*	*Diabetic control*	*DC + AG (0.3% of diet)*	*DC + SM-L (0.1% of diet)*	*DC + SM-H (0.3% of diet)*
Physical and biochemical parameters					
Body weight (g)	453 ± 34	297 ± 31^{a}	309 ± 56^{a}	308 ± 79^{a}	348 ± 55^{a}
Fluid intake (ml/day/rat)	40.3 ± 9	160 ± 16^{a}	149 ± 23^{a}	161 ± 6^{a}	150 ± 8^{a}
Plasma glucose (mg/dl)	98.3 ± 17.9	471 ± 61^{a}	461 ± 53^{a}	504 ± 52^{a}	396 ± 31^{a}
HbA_{1c} (%)	3.2 ± 0.2	11.2 ± 0.5^{a}	10.8 ± 0.5^{a}	11.7 ± 0.8^{a}	10.3 ± 0.6^{a}
Urinary albumin excretion (mg/24 h)	5.0 ± 3.9	63.7 ± 15.8^{a}	51.5 ± 37.7^{a}	50.9 ± 19.5^{a}	43.6 ± 12.3^{a}
Oxidative biomarkers					
8-Isoprostane (mg/ml)	14.4 ± 5.6	29.7 ± 8.9^{a}	—	25.7 ± 6.3^{a}	17.4 ± 6.0^{b}
Carbonyl protein (%)	36.5 ± 7.2	100 ± 8.8^{a}	—	$76.6 \pm 6.4^{a,b}$	$72.9 \pm 12.5^{a,b}$
Lymphocyte DNA damage (tail DNA%)	3.0 ± 0.9	17.7 ± 1.8^{a}	$13.1 \pm 1.7^{a,b}$	16.7 ± 1.3^{a}	$13.0 \pm 2.0^{a,b}$
Erythrocyte hemolysis (%)	—	100 ± 7.0	—	95.5 ± 15.0^{a}	$80.4 \pm 12.0^{a,b}$
Inflammatory biomarkers					
Tumor necrosis factor-α (pg/ml)	22.8 ± 3.7	90.2 ± 11.1^{a}	$52.5 \pm 7.6^{a,b}$	83.7 ± 8.8^{a}	$69.6 \pm 7.5^{a,b}$
Nitric oxide (nM)	16.9 ± 6.9	72.2 ± 6.8^{a}	$27.7 \pm 3.4^{a,b}$	$54.2 \pm 10.2^{a,b}$	$41.9 \pm 12.4^{a,b}$

Values are given as the means ± SD for 8–10 rats in each group.
[a] $p < 0.05$ *versus* nondiabetic control.
[b] $p < 0.05$ *versus* diabetic control.
AG, aminoguanidine; SM, silymarin.

Glycative biomarkers in experimental rats

The diabetic animals had significant increases in the tail tendon breaking times (Fig. 7; upper panel), development of AGE-related fluorescence (Fig. 7; middle panel), and levels of plasma albumin AGEs (Fig. 7; bottom panel) compared with NC group ($p < 0.05$). The inhibitory effects on either parameter were noted with all of the treatment regimens except the SM-L group, which had no significant effect on the inhibition of AGE-related fluorescence compared with the DC group (Fig. 7; $p > 0.05$).

AGE immunohistochemistry and immunoblotting

The monoclonal antibody raised against AGEs (6D12) was used for the immunohistochemical analysis and western blotting of the Maillard reaction products in the experimental rats. The specificity of the antibody was tested by preincubation with free antigens. As a result, no positive staining was observed after such preincubation (data not shown). Figure 8 shows immunohistochemical staining for AGEs in the aortas and renal glomeruli. With diabetes, AGEs were primarily localized in the extracellular matrix surrounding the smooth muscle cells of the aorta (Fig. 8A) and were also intensified in the glomeruli of the kidney (Fig. 8B). AG or SM-H treatment reduced the labeling of AGEs in the aortas and glomeruli of diabetic rats. Subsequent immunoblotting analysis the formation of AGEs showed similar results. The formation and accumulation of AGEs in the aortas (Fig. 8C, $p < 0.05$) and kidneys (Fig. 8D, $p < 0.05$) were increased in the DC group compared with the NC group. SM treatment was associated with reduced formation of AGEs in both of the diabetic treatment groups (SM-L and SM-H) as compared with their untreated counterparts. The AG-treated group had the most potent decrease in the formation of AGEs in the organs mentioned above (Fig. 8C, D).

Discussion

In this study, the phenomenon of protein glycation was demonstrated in the reaction mixtures of albumin with sugar by several model systems *in vitro*. Sugars, including glucose, δ-Glu, and ribose, in addition to a dicarbonyl compound, such as MG, were used as glycated agents, which are commonly adopted in Maillard reaction-associated studies (18, 29, 38). Human hemoglobin, BSA, and G.K. peptides, representing the amine sources serve as targets for glycated agents although G.K. peptides are not found in physiology or food systems (13, 32). These experimental methods uniquely differentiate between specific inhibitors of the early stage (Amadori products), middle stage (RCS), and the last stage of glycation (formation and crosslinking of AGEs) (18, 32). Our results revealed that SM inhibited AGE-related fluorescence, RCS-derived protein modifications, and the generation of ROS during glycation process (Figs. 1 and 2). A high correlation was proposed between antioxidant capacity and antiglycation action of SM. To the best of our knowledge, this is the first report showing SM as a potential anti-AGE agent.

There is positive feedback in the pathogenetic mechanism of glycation; ROS increase the formation of AGEs, the process being termed glycoxidation or autoxidative glycation (41). Owing to these adverse conditions, a supplement of antioxidants in response to protein glycation should be a theoretical strategy for preventing diabetic complications (1, 2). Having available clinical and experimental information, it may be of great interest to propose that administration of antioxidant flavonoids may be beneficial for the prevention of protein glycation. Daflon 500, a clinical drug that is composed of

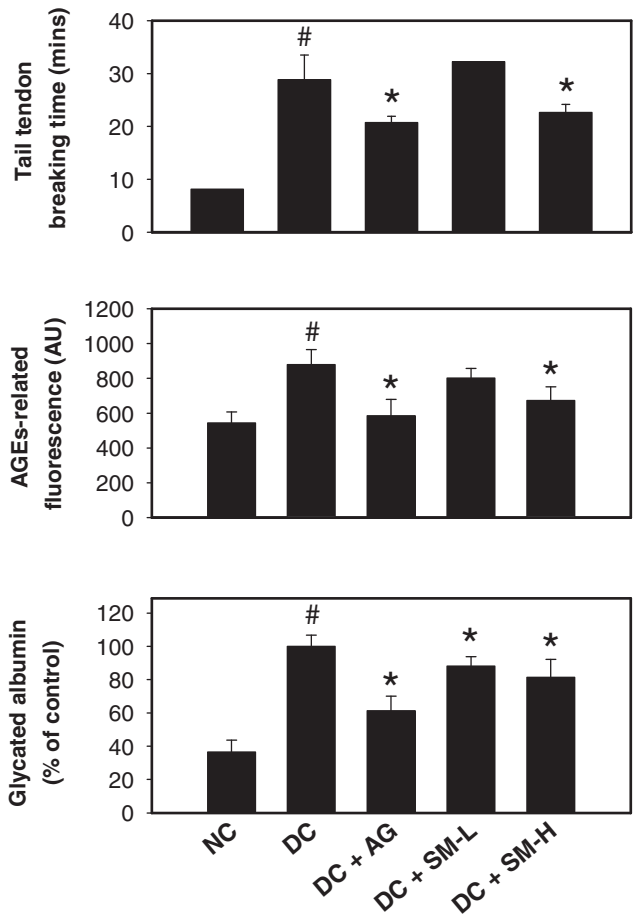

FIG. 7. Effects of SM and AG on plasma AGEs and tail collagen crosslinking in experimental rats. Tendon breaking time measured in the tail tendons of experimental rats (*upper panel*). AGE-related fluorescence at 370/440 nm corrected for protein content. The fluorescence intensity was expressed in AU (*middle panel*). Plasma-glycated albumin levels were estimated by Glycalbumin ELISA kits using a monoclonal antibody (A717) that specifically recognizes the glycated moieties in glycated albumin. Glycated albumin values were expressed relative to total albumin content after determination of total plasma albumin (*bottom panel*). Data are given as means ± SD for 8 to 10 rats in each group. $^{\#}p < 0.05$ compared with the NC group. $^{*}p < 0.05$ compared with the DC group. AU, arbitrary units; DC, diabetic control; NC, nondiabetic control.

flavonoids, has attenuated effects on HbA_{1C} levels and protein glycation in a group of 28 type 1 diabetic patients (21). Phytoestrogenic isoflavonoids, such as daidzein and genistein, have been shown to interfere with AGE-mediated oxidative DNA damage in hypertensive rats, which is attributed to direct scavenging action on AGE-derived radicals (25). Antiglycation candidates, such as green tea extract (30) and tomato paste fraction (18), are also related to their flavonoid contents in a similar system.

Increasing evidence points to the adverse effects of AGEs that are mediated by ligation of the RAGE. Aside from AGEs, several short peptides, such as S100b, can also upregulate RAGE expression, rendering the cells more susceptible to the effects of AGEs. Accordingly, S100b serves as a valuable tool in the study of AGEs and RAGE signaling in diabetic inflammatory conditions (9, 35). Because circulating monocytes are continuously exposed to conditions of high AGEs in diabetes, we examined if SM influenced S100b-driven oxidative stress and inflammatory responses in monocytes. The results may provide additional information to better understand the beneficial effects of SM in situations where either AGEs accumulate or NF-κB regulation of RAGE is activated.

In the present study, we have focused on S100b-stimulated monocytes in which a large panel of NF-κB-responsive genes, including IL-1β, was enhanced. Interestingly, we observed that SM was potent in inhibiting S100b-induced IL-1β activation (Fig. 3). Dasu *et al.* (4) reported that hyperglycemic conditions led to ROS and release of inflammatory mediators from monocytes that interfere with mitogen-activated protein kinases, protein kinase C, and NADPH oxidase. Further, the underlying mechanism was suggested to be an increase in the activation of an ROS-dependent NF-κB cascade. Similar results were obtained in the present study with S100b stimuli (Fig. 4). The SM-related decrease in IL-1β release from monocytes was likely through the abolishment of NADPH oxidase-associated p47phox expression (Fig. 4C). This process may mediate the ROS formation resulting in NF-κB-dependent genes expression. Indeed, the results indicated that S100b evoked IL-1β production, which was associated with increased recruitment of the CBP and CARM1 coactivators and p65 to the IL-1β promoter (Figs. 5 and 6). Nuclear acetylation controlled by histone acetylase and histone deacetylase (23) as well as methylation controlled by several site-specific methyltransferase, such as CARM1 (20, 24), are critical events during diabetes and inflammation conditions. Intrinsic histone acetylase, CBP, and CARM1 are able to acetylate and methylate histones and inflammation-responsive transcription factors (24). Among the histone modifications, we have observed that acetylation of HH3 at Lys9 and/or Lys14 and methylation of HH3 at Arg17 were associated with IL-1β gene activation in response to S100b stimulation (Fig. 6). However, despite S100b induction of nuclear NF-κB, CBP, and CARM1 in monocytic cells, the treatment of SM prevented the recruitment of these coactivators to their respective sites on the promoter. SM interfered with S100b-induced histone acetylation and methylation surrounding the IL-1β promoter, which provided an explanation for the abolished to recruit transcription factor NF-κB.

In this work, we further reported the influence of SM on the levels of AGEs in experimental diabetic rats. Previously, we have screened a series of polyphenol antioxidants, including 10 flavonoids (43, 45), 12 phenolic acids (46), curcumin, and SM to evaluate their effects on protein glycation, crosslinking, and subsequent formation of AGEs to find promising candidates as anti-AGE agents for further investigation. Two of these polyphenol compounds had consistent evidence of inhibitory activities toward the formation of AGEs in streptozotocin-induced insulin-deficient diabetic rats (Supplemental Material; *see* www.liebertonline.com/ars). One of the candidate compounds, SM, displayed powerful inhibitory activity of AGEs and was more or equally effective compared with the activity of pharmacological AG. In this study, diabetic rats were given SM (0.1% and 0.3% of diet) for a period of 12 weeks. The oxidative stress and inflammatory responses observed in diabetic rats were significantly reduced by SM administration (Table 1). The accelerated accumulation of AGEs

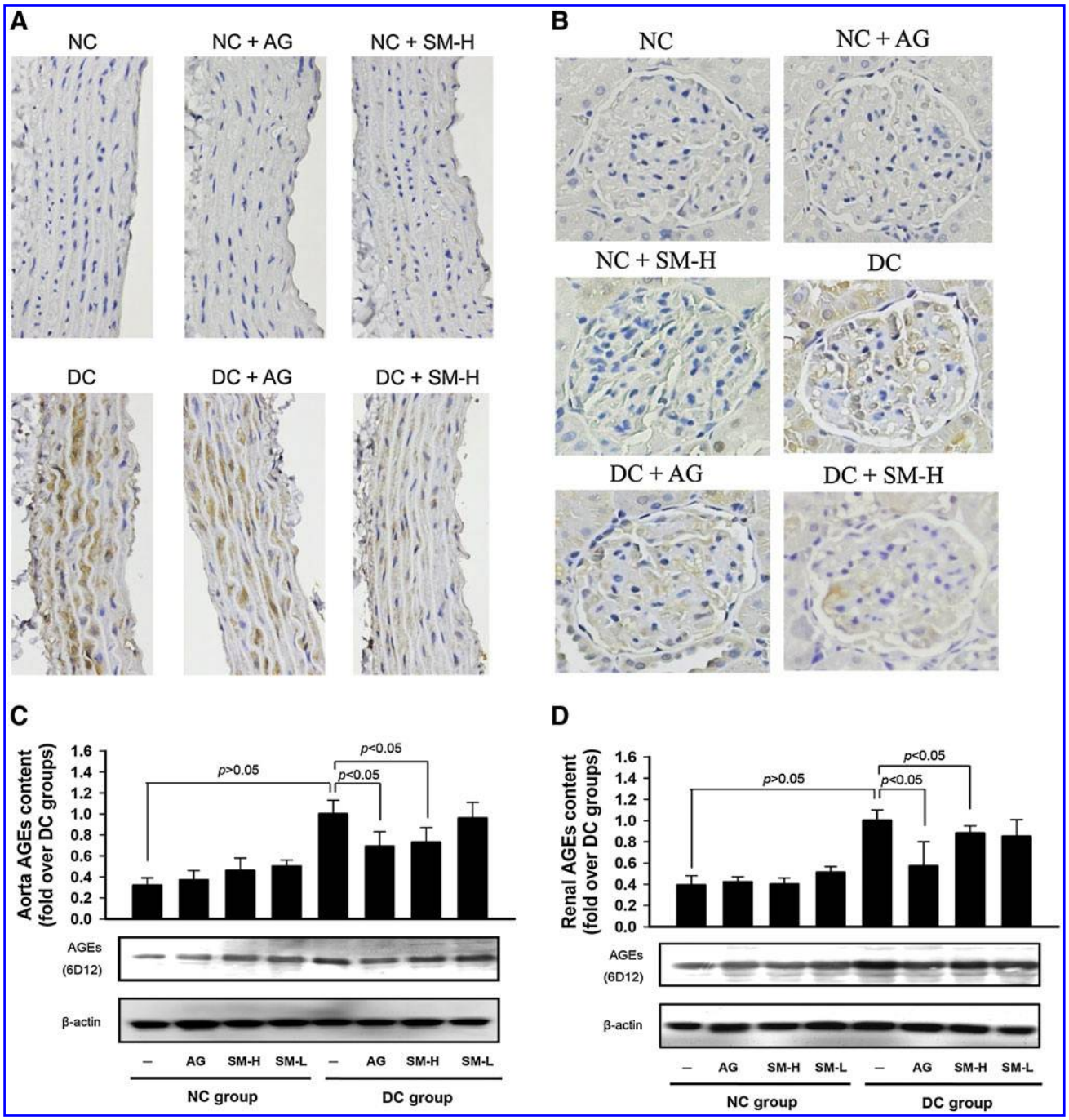

FIG. 8. SM and AG inhibit the formation of AGEs in experimental rats. The immunohistochemical staining of the AGEs in aortas (**A**) and renal glomeruli (**B**) at week 12 is shown with original magnification (400×). Western blots showing that the increased formation of AGEs in the aorta (**C**) and renal (**D**) was significantly reduced by SM or AG treatments. Results were quantified using a densitometer for 8 to 10 rats in each group. $^{\#}p < 0.05$ compared with the NC group. $^{*}p < 0.05$ compared with the DC group. (For interpretation of the references to color in this figure legend, the reader is referred to the web version of this article at www.liebertonline.com/ars).

and the crosslinking of tail tendon collagen in diabetic rats were also prevented to a greater extent by SM treatment (Figs. 7 and 8). The results allow us to confirm that SM has an inhibitory effect on glycation and subsequent crosslinking *in vivo*. However, the nonsignificant effect of SM on hyperglycemia and HbA_{1c} levels in diabetic rats observed in this study, which was contrary to a recent report on the adjunct use of SM with glibenclamide, improved the glycemic control. This effect on glycemic control may be related to increased insulin sensitivity in peripheral tissues (16). As SM treatment reduced the increased oxidant damage and inflammation in diabetic animals, serum albumin in these animals was exposed to the same amount of hyperglycemia and for the same duration as in untreated diabetic control animals (DC group), but in a reduced oxidative stress and inflammatory environment. This underscored the significance of oxygen radicals

and proinflammatory cytokines in the formation of AGEs *in vivo*. As ROS initiates a vicious cycle in which the levels of AGEs and inflammatory mediators are persistent increased in diabetic conditions, the antioxidant and antiinflammatory properties of SM may play a vital role in its antiglycation action.

In conclusion, SM has potent inhibitory effects on protein glycation and the subsequent formation of AGEs. SM also targets the chromatin remodeling machinery to prevent inflammatory mediators transcription. Further, this study confirms the significance of oxidative stress and inflammation in the accumulation of AGEs in diabetes, and it supports SM administration for the prevention of glycotoxin-associated complications of diabetes mellitus.

Acknowledgments

This research work was partially supported by the National Science Council, NSC94-2321-B005-001 and NSC96-2628-B005-004-MY3, Taiwan, Republic of China. The authors also would like to thank Dr. J. W. Liao of the Graduate Institute of Veterinary Pathobiology for his technical assistance on immunohistochemical staining.

Author Disclosure Statement

The authors declare no conflicts of interest in this work.

References

1. Bonnefont-Rousselot D. Antioxidant and anti-AGE therapeutics: evaluation and perspectives. *J Soc Bio* 195: 391–398, 2001.
2. Bonnefont-Rousselot D. Glucose and reactive oxygen species. *Curr Opin Clin Nutr Metab Care* 5: 561–568, 2002.
3. Cohen MP. Intervention strategies to prevent pathogenetic effects of glycated albumin. *Arch Biochem Biophys* 419: 25–30, 2003.
4. Dasu MR, Devaraj S, and Jialal I. High glucose induces IL-1beta expression in human monocytes: mechanistic insights. *Am J Physiol Endocrinol Metab* 293: E337–E346, 2007.
5. Day JF, Thorpe SR, and Baynes JW. Nonenzymatically glucosylated albumin. *In vitro* preparation and isolation from normal human serum. *J Biol Chem* 254: 595–597, 1979.
6. Devaraj S, Venugopal SK, Singh U, and Jialal I. Hyperglycemia induces monocytic release of interleukin-6 via induction of protein kinase C-α and -β. *Diabetes* 54: 85–91, 2005.
7. Donato R. RAGE: a single receptor for several ligands and different cellular responses: the case of certain S100 proteins. *Curr Mol Med* 7: 711–724, 2007.
8. Figarola JL, Loera S, Weng Y, Shanmugam N, Natarajan R, and Rahbar S. LR-90 prevents dyslipidaemia and diabetic nephropathy in the Zucker diabetic fatty rat. *Diabetologia* 51: 882–891, 2008.
9. Figarola JL, Shanmugam N, Natarajan R, and Rahbar S. Anti-inflammatory effects of the advanced glycation end product inhibitor LR-90 in human monocytes. *Diabetes* 56: 647–655, 2007.
10. Finotti P, Pagetta A, and Ashton T. The oxidative mechanism of heparin interferes with radical production by glucose and reduces the degree of glycooxidative modifications on human serum albumin. *Eur J Biochem* 268: 2193–2200, 2001.
11. Forbes JM, Cooper ME, Thallas V, Burns WC, Thomas MC, Brammar GC, Lee F, Grant SL, Burrell LA, Jerums G, and Osicka TM. Reduction of the accumulation of advanced glycation end products by ACE inhibition in experimental diabetic nephropathy. *Diabetes* 51: 3274–3282, 2002.
12. Guha M, Bai W, Nadler JL, and Natarajan R. Molecular mechanisms of tumor necrosis factor alpha gene expression in monocytic cells via hyperglycemia-induced oxidant stress-dependent and -independent pathways. *J Biol Chem* 275: 17728–17739, 2000.
13. Hayashi T, Ohta Y, and Namiki M. Electron spin resonance spectral study on the structure of the novel free radical products formed by the reactions of sugars with amino acids or amines. *J Agric Food Chem* 25: 1282–1287, 1977.
14. Hipkiss AR, Brownson C, and Carrier MJ. Carnosine the anti-ageing anti-oxidant dipeptide may react with protein carbonyl groups. *Mech Ageing Dev* 122: 1431–1445, 2001.
15. Hortelano S, Dewez B, Genaro AM, Díaz-Guerra MJ, and Boscá L. Nitric oxide is released in regenerating liver after partial hepatectomy. *Hepatology* 21: 776–786, 1995.
16. Hussain SA. Silymarin as an adjunct to glibenclamide therapy improves long-term and postprandial glycemic control and body mass index in type 2 diabetes. *J Med Food* 10: 543–547, 2007.
17. Khalifah RG, Chen Y, and Wassenberg JJ. Post-Amadori AGE inhibition as a therapeutic target for diabetic complications: a rational approach to second-generation Amadorin design. *Ann NY Acad Sci* 1043: 793–806, 2005.
18. Kiho T, Usui S, Hirano K, Aizawa K, and Inakuma T. Tomato paste fraction inhibiting the formation of advanced glycation end-products. *Biosci Biotechnol Biochem* 68: 200–205, 2004.
19. Lee C, Yim MB, Chock, PB, Yim HS, and Kang SO. Oxidation-reduction properties of methylglyoxal-modified protein in relation to free radical generation. *J Biol Chem* 273: 25272–25278, 1998.
20. Li Y, Reddy MA, Miao F, Shanmugam N, Yee JK, Hawkins D, Ren B, and Natarajan R. Role of the histone H3 lysine 4 methyltransferase SET7/9 in the regulation of NF-kappaB-dependent inflammatory genes. Relevance to diabetes and inflammation. *J Biol Chem* 283: 26771–26781, 2008.
21. Manuel Y, Keenoy B, Vertommen J, and De Leeuw I. The effect of flavonoid treatment on the glycation and antioxidant status in Type 1 diabetic patients. *Diabetes Nutr Metab* 12: 256–263, 1999.
22. Martinez-Florez S, Gonzalez-Gallego J, Culebras JM, and Tunon MJ. Flavonoids: properties and anti-oxidizing action. *Nutr Hosp* 17: 271–278, 2002.
23. Miao F, Gonzalo IG, Lanting L, and Natarajan R. *In vivo* chromatin remodeling events leading to inflammatory gene transcription under diabetic conditions. *J Biol Chem* 279: 18091–18097, 2004.
24. Miao F, Li S, Chavez V, Lanting L, and Natarajan R. Coactivator-associated arginine methyltransferase-1 enhances nuclear factor-kappaB-mediated gene transcription through methylation of histone H3 at arginine 17. *Mol Endocrinol* 20: 1562–1573, 2006.
25. Mizutani K, Ikeda K, Nishikata T, and Yamori Y. Phytoestrogens attenuate oxidative DNA damage in vascular smooth muscle cells from stroke-prone spontaneously hypertensive rats. *J Hypertens* 18: 1833–1840, 2000.
26. Montonen J, Knekt P, Jarvinen R, and Reunanen A. Dietary antioxidant intake and risk of type 2 diabetes. *Diabetes Care* 27: 362–366, 2004.
27. Münch G, Keis R, Wessels A, Riederer P, Bahner U, Heidland A, Niwa T, Lemke HD, and Schinzel R. Determination of advanced glycation end products in serum by fluorescence

spectroscopy and competitive ELISA. *Eur J Clin Chem Clin Biochem* 35: 669–677, 1997.
28. Nagaraj RH, Shipanova IN, and Faust FM. Protein cross-linking by the Maillard reaction: Isolation characterization and *in vivo* detection of a lysine-lysine cross-link derived from methylglyoxal. *J Biol Chem* 271: 19338–19345, 1996.
29. Nagasawa T, Tabata N, Ito Y, Aiba Y, Nishizawa N, and Kitts DD. Dietary G-rutin suppresses glycation in tissue proteins of streptozotocin-induced diabetic rats. *Mol Cell Biochem* 252: 141–147, 2003.
30. Nakagawa T, Yokozawa T, Terasawa K, Shu S, and Juneja LR. Protective activity of green tea against free radical- and glucose-mediated protein damage. *J Agric Food Chem* 50: 2418–2422, 2002.
31. Negre-Salvayre A, Salvayre R, Augé N, Pamplona R, and Portero-Otín M. Hyperglycemia and glycation in diabetic complications. *Antioxid Redox Signal* 11: 3071–3109, 2009.
32. Rahbar S, Yerneni KK, Scott S, Gonzales N, and Lalezari I. Novel inhibitors of advanced glycation endproducts (part II). *Mol Cell Biol Res Commun* 3: 360–366, 2000.
33. Richard LR and Lloyd RV. Free radical formation from secondary amines in the Maillard reaction. *J Agric Food Chem* 45: 2413–2418, 1997.
34. Schiekofer S, Andrassy M, Chen J, Rudofsky G, Schneider J, Wendt T, Stefan N, Humpert P, Fritsche A, Stumvoll M, Schleicher E, Häring HU, Nawroth PP, and Bierhaus A. Acute hyperglycemia causes intracellular formation of CML and activation of ras p42/44 MAPK and nuclear factor kappaB in PBMCs. *Diabetes* 52: 621–633, 2003.
35. Shanmugam N, Kim YS, Lanting L, and Natarajan R. Regulation of cyclooxygenase-2 expression in monocytes by ligation of the receptor for advanced glycation end products. *J Bio Chem* 278: 34834–34844, 2003.
36. Shanmugam N, Reddy MA, Guha M, and Natarajan R. High glucose-induced expression of proinflammatory cytokine and chemokine genes in monocytic cells. *Diabetes* 52: 1256–1264, 2003.
37. Shih PH, Yeh CT, and Yen GC. Anthocyanins induce the activation of phase II enzymes through the antioxidant response element pathway against oxidative stress-induced apoptosis. *J Agric Food Chem* 55: 9427–9435, 2007.
38. Thornalley PJ, Langborg A, and Minhas HS. Formation of glyoxal methylglyoxal and 3-deoxyglucosone in the glycation of proteins by glucose *Biochem J* 344: 109–116, 1999.
39. Thornalley PJ. Use of aminoguanidine (Pimagedine) to prevent the formation of advanced glycation endproducts. *Arch Biochem Biophys* 419: 31–40, 2003.
40. Venugopal SK, Devaraj S, Yang T, and Jialal I. Alpha-tocopherol decreases superoxide anion release in human monocytes under hyperglycemic conditions via inhibition of protein kinase C-alpha. *Diabetes* 51: 3049–3054, 2002.
41. Wolff SP and Dean RT. Glucose autoxidation and protein modification. *Biochem J* 245: 243–250, 1987.
42. Woodside JV, Yarnell JW, McMaster D, Young IS, Harmon DL, McCrum EE, Patterson CC, Gey KF, Whitehead AS, and Evans A. Effect of B-group vitamins and antioxidant vitamins on hyperhomocysteinemia: a double-blind randomized factorial-design controlled trial. *Am J Clin Nutr* 67: 858–866, 1998.
43. Wu CH and Yen GC. Inhibitory effect of naturally occurring flavonoids on advanced glycation endproducts formation. *J Agric Food Chem* 53: 3167–3173, 2005.
44. Wu CH, Hsieh CL, Song TY, and Yen GC. Inhibitory effects of *Cassia tora* L. on benzo[*a*]pyrene-mediated DNA damage toward HepG2 cells. *J Agric Food Chem* 49: 2579–2586, 2001.
45. Wu CH, Wu CF, Huang HW, Jao YC, and Yen GC. Naturally occurring flavonoids attenuate high glucose-induced expression of proinflammatory cytokines in human monocytic THP-1 cells. *Mol Nutr Food Res* 53: 984–995, 2009.
46. Wu CH, Yeh CT, Shih PH, and Yen GC. Dietary phenolic acids attenuate multiple stages of protein glycation and high-glucose-stimulated proinflammatory IL-1beta activation by interfering with chromatin remodeling and transcription in monocytes. *Mol Nutr Food Res* 54: 1–14, 2010.
47. Wu JW, Lin LC, and Tsai TH. Drug-drug interactions of silymarin on the perspective of pharmacokinetics. *J Ethnopharmacol* 121: 185–193, 2009.
48. Yue DK, McLennan S, Delbridge L, Handelsman DJ, Reeve T, and Turtle JR. The thermal stability of collagen in diabetic rats: correlation with severity of diabetes and non-enzymatic glycosylation. *Diabetologia* 24: 282–285, 1983.

Address correspondence to:
Dr. Gow-Chin Yen
Department of Food Science and Biotechnology
National Chung Hsing University
250 Kuokuang Road
Taichung 40227
Taiwan

E-mail: gcyen@nchu.edu.tw

Date of first submission to ARS Central, February 3, 2010; date of final revised submission, June 24, 2010; date of acceptance, June 25, 2010.

Abbreviations Used

AG = aminoguanidine
AGEs = advanced glycation end products
APO = apocynin
BSA = bovine serum albumin
CARM1 = coactivator-associated arginine methyltransferase-1
CBP = CREB-binding protein
ChIP = chromatin immunoprecipitation
CREB = cAMP response element-binding
EGFR = epidermal growth factor receptor
ESR = electron spin resonance
G.K. peptide = *N*-acetyl-glycyl-lysine methyl ester peptide
HG = high glucose
HH3(4) = histone 3(4)
IL-1β = interleukin-1β
MG = methylglyoxal
NF-κB = nuclear factor-kappaB
NO = nitric oxide
RAGE = receptor for advanced glycation end products
RCS = reactive carbonyl species
ROS = reactive oxygen species
RT-PCR = real-time polymerase chain reaction
SDS-PAGE = sodium dodecyl sulphate-polyacrylamide gel electrophoresis
SM = silymarin
STZ = streptozotocin
TNF-α = tumor necrosis factor-α

This article has been cited by:

1. An-Sheng Cheng, Yu-Hsiang Cheng, Chiu-Hsia Chiou, Tsu-Liang Chang. 2012. Resveratrol Upregulates Nrf2 Expression To Attenuate Methylglyoxal-Induced Insulin Resistance in Hep G2 Cells. *Journal of Agricultural and Food Chemistry* **60**:36, 9180-9187. [CrossRef]
2. Bao-Hong Lee, Wei-Hsuan Hsu, Yu-Ying Chang, Hsuan-Fu Kuo, Ya-Wen Hsu, Tzu-Ming Pan. 2012. Ankaflavin: A natural novel PPAR# agonist up-regulated Nrf2 to attenuate methylglyoxal (MG)-induced diabetes in vivo. *Free Radical Biology and Medicine* . [CrossRef]
3. Mohammad Kazem Fallahzadeh, Banafshe Dormanesh, Mohammad Mahdi Sagheb, Jamshid Roozbeh, Ghazal Vessal, Maryam Pakfetrat, Yahya Daneshbod, Eskandar Kamali-Sarvestani, Kamran B. Lankarani. 2012. Effect of Addition of Silymarin to Renin-Angiotensin System Inhibitors on Proteinuria in Type 2 Diabetic Patients With Overt Nephropathy: A Randomized, Double-Blind, Placebo-Controlled Trial. *American Journal of Kidney Diseases* . [CrossRef]
4. Abdullah Acar, Esref Akil, Harun Alp, Osman Evliyaoglu, Erkan Kibrisli, Ali Inal, Fatma Unan, Nebahat Tasdemir. 2012. Oxidative Damage is Ameliorated by Curcumin Treatment in Brain and Sciatic Nerve of Diabetic Rats. *International Journal of Neuroscience* **122**:7, 367-372. [CrossRef]
5. Jer-An Lin, Chi-Hao Wu, Song-Chwan Fang, Gow-Chin Yen. 2012. Combining the observation of cell morphology with the evaluation of key inflammatory mediators to assess the anti-inflammatory effects of geranyl flavonoid derivatives in breadfruit. *Food Chemistry* . [CrossRef]
6. Chi-Hao Wu, Shang-Ming Huang, Jer-An Lin, Gow-Chin Yen. 2011. Inhibition of advanced glycation endproduct formation by foodstuffs. *Food & Function* **2**:5, 224. [CrossRef]